

Supplementary Information

Protein folding stability changes across the proteome

reveal targets of Cu toxicity in *E. coli*

Nancy Wiebelhaus¹, Jacqueline M. Zaengle-Barone¹, Kevin K. Hwang, Katherine J. Franz*, Michael C. Fitzgerald*

¹These authors contributed equally to the work.

*Corresponding authors: katherine.franz@duke.edu, michael.c.fitzgerald@duke.edu

Department of Chemistry, Duke University, 124 Science Drive, Durham, North Carolina 27708, United States

The supplementary information accompanying this manuscript includes Supplementary Text, 5 Supplementary Tables, 6 Supplementary Figures, and 8 Supplementary Datasets as summarized below:

Table of Contents

Supplementary Text | Description of Materials and Methods

Supplementary Table 1 | Proteomic coverage from protein expression level and protein stability analyses.

Supplementary Table 2 | Complete list of protein expression level hits.

Supplementary Table 3 | Complete list of protein stability hits.

Supplementary Table 4 | Biological process classification of protein stability hits.

Supplementary Table 5 | Biological process classification of protein stability hits within each cluster.

Supplementary Figure 1 | Electron paramagnetic resonance spectroscopy of Cu titrated with PT in 10% glycerol.

Supplementary Figure 2 | Experimental workflow and isobaric mass tagging scheme for protein expression analysis.

Supplementary Figure 3 | Experimental workflow and isobaric mass tagging scheme for protein stability analysis.

Supplementary Figure 4 | Heat map visualizing magnitude of expression changes for hit proteins grouped by biological process.

Supplementary Figure 5 | Heat maps visualizing magnitude of stability changes for hit peptides grouped by biological process.

Supplementary Figure 6 | GAPDH and IDH activity in cells treated with PT.

- Supplementary Dataset 1 | Search output and $\log_2(\text{fold change})$ calculations from LC-MS/MS analyses of the first TMT10-plex labeled sample generated in the protein expression level analyses (i.e., biological replicates 1 and 2).
- Supplementary Dataset 2 | Search output and $\log_2(\text{fold change})$ calculations from LC-MS/MS analyses of the second TMT10-plex labeled sample generated in the protein expression level analyses (i.e., biological replicates 3 and 4).
- Supplementary Dataset 3 | Search output and $\log_2(\text{fold change})$ calculations from LC-MS/MS analyses of the first TMT10-plex labeled sample generated in the protein stability analyses (i.e., biological replicates 1 and 2).
- Supplementary Dataset 4 | Search output and $\log_2(\text{fold change})$ calculations from LC-MS/MS analyses of the first TMT10-plex labeled sample generated in the protein stability analyses (i.e., biological replicates 3 and 4).
- Supplementary Dataset 5 | Hit analysis of overlapping proteins identified in the two TMT10-plex labeled samples generated in the protein expression level analyses (i.e., biological replicates 1-4).
- Supplementary Dataset 6 | Hit analysis of overlapping proteins identified in the two TMT10-plex samples generated in the protein stability analyses (i.e., biological replicates 1-4).
- Supplementary Dataset 7 | Fuzzy c-means cluster analysis of peptide stability hits.
- Supplementary Dataset 8 | DAVID functional analysis and resulting GO biological process classifications of protein expression level hits and proteins corresponding to peptide stability hits.

SUPPLEMENTARY TEXT

MATERIALS & METHODS

Materials. The following materials were obtained from Sigma Aldrich (St. Louis, MO): dimethyl sulfoxide (DMSO), phenylmethanesulfonyl fluoride (PMSF), S-methylmethanethiosulfonate (MMTS), sodium chloride, ethylenediaminetetraacetic acid (EDTA), urea, centrifugal filter units (Amicon Ultra, 0.5 mL, 10k molecular weight cutoff), tris(hydroxymethyl)aminomethane hydrochloride (Tris-HCl), thermolysin from *Geobacillus stearothermophilus*, trifluoroacetic acid (TFA), triethylammonium bicarbonate buffer (TEAB, 1 M, pH 8.5), LB medium (Lennox), glyceraldehyde-3-phosphate dehydrogenase from rabbit muscle, isocitrate dehydrogenase (NADP) from porcine heart, DL-glyceraldehyde-3-phosphate, DL-isocitric acid trisodium salt hydrate, and β -nicotinamide adenine dinucleotide phosphate sodium salt hydrate. The following materials were obtained from Thermo Fisher Scientific (Waltham, MA): acetonitrile (ACN, LC-MS grade), trace metal-grade nitric acid, TMT10-Plex isobaric label reagent set, NHS-activated agarose dry resin (Pierce), Coomassie Plus Bradford Reagent (Pierce), and porcine pancreas trypsin (proteomics grade). Tris(2-carboxyethyl)phosphine hydrochloride (TCEP) was obtained from Santa Cruz Biotechnology (Dallas, TX). Phosphate-buffered saline (PBS 1x, without calcium or magnesium, pH 7.4) and ethylenediaminetetraacetic acid (EDTA) solution (0.5 M, pH 8.0) were obtained from Corning (Corning, NY). Macrospin columns (silica C18) were obtained from Nest Group (Southborough, MA). β -Nicotinamide adenine dinucleotide and pyriothione were obtained from Chem-Impex International. Copper chloride was obtained from Merck. Incorporation of β -lactamase CTX-M-1 into *E. coli* strain K-12 MG1655 and synthesis of PcephPT (2-((((6R,7R)-2-carboxy-8-oxo-7-(2-phenylacetamido)-5-thia-1-azabicyclo[4.2.0]oct-2-en-3-yl)methyl)thio)pyridine 1-oxide) were described previously.¹

Treatment and preparation of *E. coli* for inductively coupled plasma mass spectrometry (ICP-MS). *E. coli* MG1655 expressing β -lactamase CTX-M-1 was streaked onto LB agar containing 100 μ g/mL ampicillin and 50 μ g/mL kanamycin. A single colony was used to inoculate 7–9 mL LB medium containing 100 μ g/mL ampicillin and 50 μ g/mL kanamycin, which was then incubated at 37 °C, 200 rpm, for 16–18 h. This overnight culture was diluted 1:100 in LB medium and grown to OD₆₀₀ of 0.1–0.2. The culture was then divided into 100 mL aliquots and treated with nothing, 10 μ M CuCl₂, 4 μ M PT, 4 μ M PcephPT, 10 μ M Cu + 4 μ M PT, 10 μ M Cu + 4 μ M PcephPT, or 2 mM Cu for 15 min. Then, 5 mL of cell suspension was placed in acid-washed centrifuge tubes and centrifuged at 4000 g, 4 °C for 10 min to pellet. Pellets were washed twice with 1 mL sterile H₂O and once with 1 mL of 1 mM EDTA to remove extracellular metals, then dried at 80–90 °C overnight. After drying, samples were digested in 30 μ L of neat trace metal-grade nitric acid at 80–90 °C for 30 min, then allowed to cool. Next, 30 μ L of chelex-treated water was added to obtain a final nitric acid concentration of 50%. Samples were stored at -20 °C until submission for ICP-MS analysis. Two biological replicates were performed, each with two technical replicates. ICP-MS data were acquired by Kim Hutchison of the North Carolina State University Department of Crop and Soil Sciences using a PerkinElmer Elan DRCII spectrometer. The concentration of Cu per cell was determined by dividing the number of cells in the sample by the volume of an *E. coli* MG1655 cell cultured in LB media (3.9×10^{-15} L).²

Treatment and preparation of *E. coli* for electron paramagnetic resonance (EPR) spectroscopy. The growth culture of *E. coli* MG1655 CTX-M-1 was obtained as described above for ICP-MS. Cells were grown to an OD₆₀₀ of 0.8–1, divided into 100 mL aliquots, and treated for 15 min. The cells were then centrifuged at 4000 g for 10 min at 4 °C to pellet. Pellets were washed

twice with 5 mL sterile water and once with 5 mL of 1 mM EDTA, then resuspended in 10% glycerol. Hydrogen peroxide (1 M) and hydroxylamine (1 mM) were added to one set of the samples to allow comparison between oxidized and unoxidized metal content. Hydroxylamine was added 15 min before hydrogen peroxide as a catalase inhibitor to prevent formation of bubbles upon addition of hydrogen peroxide. X-band continuous wave EPR spectroscopy was conducted on a Bruker ESP 300 spectrometer equipped with an Oxford Instruments ESR 910 continuous helium flow cryostat. Experiments were conducted at 77 K, 9.38 GHz, 20 mW microwave power, and 5 G modulation amplitude.

Microdilution experiments. Minimum inhibitory concentrations (MICs) were determined as described previously.¹ Briefly, an overnight culture was diluted 1:500 in fresh LB medium and added to a 96-well plate containing CuCl₂ serially diluted two-fold in LB medium, giving a final inoculum dilution of 1:1000 (5×10^5 to 1×10^6 CFU/mL). Plates were covered with AeraSeal film (Sigma-Aldrich) and incubated for 20 h at 37 °C, 200 rpm. Bacterial growth was evaluated by visual inspection corroborated by measuring the optical density at 600 nm (OD₆₀₀) using a Perkin Elmer Victor³ V multilabel plate reader at 0 and 20 h. The MIC was defined as the concentration at which no detectable growth occurred after 20 h of incubation. At least two biological replicates were performed with a minimum of at least four total technical replicates.

Treatment of *E. coli* and cell lysis for proteomics. The growth culture of *E. coli* MG1655 CTX-M-1 (OD₆₀₀ of 0.1–0.2) was obtained as described above for ICP-MS. The culture was then divided into 100 mL aliquots and treated with 4 μL DMSO, 10 μM CuCl₂ + 4 μL DMSO, 4 μM PT, 10 μM Cu + 4 μM PT, or 10 μM Cu + 4 μM PcephPT for 15 min. The cells were then centrifuged at 4000 g for 10 min at 4 °C to pellet. Pellets were washed twice with 5 mL sterile H₂O and stored at -20 °C until future use.

E. coli cell pellets were thawed, then lysed in 200 μL of PBS (1x, without calcium or magnesium, pH 7.4) with 1 mM PMSF. Cell lysis was accomplished by sonication at 30% amplitude for 10 seconds followed by a 50 second incubation period on ice. This was performed for a total of six cycles. The lysed cells were centrifuged at 14,000 g for 15 min at 4 °C. The total protein concentration in the supernatant from each cell lysate sample was determined by a Bradford Assay and ranged from 8–12 mg/mL. Cell lysates for each condition were normalized to 8 mg/mL before analysis by pulse proteolysis.

Protein expression workflow. Lysates generated from the *E. coli* treatment conditions previously described were also subjected to a traditional protein expression analysis. Aliquots of each lysate containing ~80 μg of protein were diluted in PBS (1x, without calcium or magnesium, pH 7.4) and transferred to 10k molecular weight cutoff centrifugal filter unit, where a filter-aided bottom-up proteomic sample preparation with isobaric mass tag labeling was employed. This involved buffer exchanging proteins into UA (0.1 M Tris, 8 M urea, pH 8.0) and reacting each sample with 100 μL of 5 mM TCEP in UA for 1 h at room temperature and subsequently with 100 μL of 20 mM MMTS in UA for 10 min at room temperature. Samples were then buffer exchanged into 0.1 M TEAB (pH 8.5) and digested with trypsin overnight at 37 °C. The ratio of trypsin to total peptide was between 1:20 and 1:100 (w/w). The digested samples were labeled with a TMT-10plex reagent kit according to the manufacturer protocol. Labeled samples were washed with 0.5 M NaCl (3x) and centrifuged through the 10k filters. Equal volumes of each TMT10-plex labeled sample were combined into one tube. This protein expression experiment was performed on five conditions with four biological replicates each, resulting in two separate TMT10-plex

labeled samples. The final combined, labeled samples were desalted using C18 Macrospin columns prior to LC-MS/MS analysis.

One-pot STEPP-PP workflow. Lysates generated from the *E. coli* treatment conditions described above were subjected to a "one-pot" pulse proteolysis (PP) analysis that included a semi-tryptic peptide enrichment strategy for proteolysis procedures (STEPP).^{3,4} The one-pot analysis employed here allowed the incorporation of two biological replicates per condition in the experiment (5 unique conditions per replicate for 10 total channels in the TMT readout). Aliquots of each lysate were distributed into a series of 12 urea-containing buffers (PBS, pH 7.4) where the final concentrations of urea were equally spaced at 0.4 M intervals between 1.0 and 5.4 M. The total amount of protein in each sample was 80 µg. The samples in the urea-containing buffers were incubated for 2 h at room temperature before 10 µg of thermolysin was added to each of the (+) and (-) ligand samples in the denaturant-containing buffers. The thermolysin proteolysis reactions proceeded for 1 min at room temperature before they were quenched upon addition of 60 µL of a urea/EDTA solution (~0.2 M EDTA, 8 M urea, pH 8.0). Equal aliquots of denaturant containing buffers from each condition in a given biological replicate were combined into a single sample, resulting in 5 combined samples representing untreated, Cu-treated, PT-treated, Cu + PT-treated, Cu + PcephPT-treated for each replicate. This ultimately generated a total of 10 samples. Aliquots containing ~90 µg of total protein from each of the 10 samples were subjected to the STEPP protocol we recently reported.³ Before the STEPP protocol, an additional 20 µL of a urea/EDTA solution (~0.2 M EDTA, 8 M urea, pH 8.0) was added to each sample to ensure proper unfolding for labeling with isobaric mass tags. As part of the STEPP protocol, samples were reacted with 1.5 mM TCEP for 1 h at 30 °C and then with 2.5 mM MMTS for 10 min at room temperature. The protein material in the 10 different samples was labeled with a TMT-10plex reagent kit according to the manufacturer's protocol. The protein samples in the 10-plex were combined to generate a single protein sample that was lyophilized, re-dissolved in 2% v/v TFA, and desalted using C18 columns according to the manufacturer's protocol. The desalted sample was lyophilized, redissolved in 0.1 M TEAB solution (pH 8.5), and digested with trypsin overnight at 37 °C. The ratio of trypsin to total peptide was between 1:20 and 1:100 (w/w). NHS-activated agarose resin and 50 µL 0.5 M NaCl was added to the digested sample, such that the NHS-activated agarose resin to total peptide ratio was approximately 150:1 (w/w). Samples were reacted for 1.5 h at room temperature, acidified with 2% v/v TFA, and transferred to C18 columns for desalting prior to LC-MS/MS analysis. This pulse proteolysis experiment was performed on five conditions with four biological replicates each, resulting in two separate TMT10-plex labeled samples for LC-MS/MS analysis.

Quantitative LC-MS/MS analysis. The LC-MS/MS analyses were performed using a nanoAcquity UPLC system (Waters) coupled to a Thermo Orbitrap Fusion Lumos mass spectrometer system. The dried peptide material generated from the first and second PP experiments were reconstituted in 12 µL and 10 µL of 1% TFA, 2% acetonitrile in H₂O, respectively. Aliquots of 1 µL and 2 µL for each experiment were injected in triplicate into the UPLC system. The dried peptide material generated from the first and second protein expression analysis were reconstituted in 30 µL and 25 µL of 1% TFA, 2% acetonitrile in H₂O, respectively. Aliquots of 1 µL and 2 µL for each sample were injected in triplicate into the UPLC system. The peptides were first trapped on a Symmetry C18 20 mm x 180 µm trapping column (5 µL/min at 99.9/0.1 water/acetonitrile, v/v). The analytical separation was performed using an Acquity 75 µm x 250 mm high strength silica (HSS) T3 C18 column with a 1.8 µm particle size (Waters); the column temperature was set to 55 °C.

Peptide elution was performed using a 90 min linear gradient of 3–30 % ACN at a flow rate of 400 nL/min. The MS data was collected using a top 20 data-dependent acquisition (DDA) method which included MS1 at 120k and MS2 at 50k resolution. The MS1 AGC target was 4.0×10^5 ions with a max injection time of 50 ms. For MS2, the AGC target was 1.0×10^5 ions with a max injection time of 105 ms. The collision energy was set to 38%, and the scan range was 375–1500 m/z. The isolation window was 0.7 and the dynamic exclusion duration was 60 s. The mass spectrometry proteomics data have been deposited to the ProteomeXchange Consortium⁵ via the PRIDE⁶ partner repository with the dataset identifier PXD021198. The raw MS data are available for confidential review using the account, reviewer79333@ebi.ac.uk, and the password, bU1driKV.

Protein expression proteomic data analysis. Proteome Discoverer 2.2 (Thermo) was used to search the raw LC-MS/MS files against the *E. coli* MG1655 (Proteome ID: UP000000625) proteins in the 2019-09-24 release of the UniProt Knowledgebase. The raw LC-MS/MS data generated in the protein expression experiments was searched using fixed MMTS modification on cysteine; TMT10-plex labeling of lysine side chains and peptide N-termini; variable oxidation of methionine; variable deamidation of asparagine and glutamine; and variable acetylation of the protein N-terminus. Trypsin (full) was set as the enzyme, and up to two missed cleavages were allowed. For peptide and protein quantification, reporter abundance was set as intensity, normalization mode and scaling mode were each set as none. All other settings were left as the default values. Only tryptic peptides with protein FDR confidence labelled as "high" or "medium" (i.e. FDR <0.01% or <0.05%) and with at least two peptides assayed were used for subsequent analyses.

For each condition (TMT-tag), a normalization factor was calculated from the average of all the intensities for that tag. The signal intensities used in the protein expression experiments were the reporter ion intensities from all the tryptic peptides for a given protein generated in Proteome Discoverer. For each identified protein in the protein expression experiment a ratio of the observed reporter ion intensities in the (+) ligand samples (Cu, PT, PT + Cu, and PcephPT + Cu treated) to the (-) ligand sample (untreated) was generated for each biological replicate. The resulting ratio was divided by the normalization factor for each of the 4 biological replicates. These normalized ratios (fold change) were then log₂-base transformed, averaged, and tested by two-tailed Student's *t*-test comparing with a mean of 0. The log₂(fold change) values of all the proteins for each comparison were used to calculate the mean log₂(fold change) and standard deviation (σ) of its distribution. Hit proteins were identified based on two criteria, (i) the protein must have a significantly altered log₂(fold change) value ($\geq 2\sigma$ deviations from mean log₂(fold change)), and (ii) the log₂(fold change) value must be significantly different from zero, as determined by a Student's two-tailed *t*-test (p -value ≤ 0.05).

One-pot STEPP-PP proteomic data analysis. The raw LC-MS/MS data generated in the PP experiments was searched using the same allowed modifications as the protein expression data. Trypsin (semi) was set as the enzyme, and up to three missed cleavages were allowed. For peptide and protein quantification, reporter abundance was set as intensity, normalization mode and scaling mode were each set as none. All other settings were left as the default values. Only semi-tryptic peptides with protein/peptide FDR confidence labelled as "high" or "medium" (i.e. FDR <0.01% or <0.05%) were used for subsequent analyses.

For each condition (TMT-tag), a normalization factor was calculated from the average of all the intensities for that tag. The signal intensities used in the PP experiments were the reporter ion intensities from the semi-tryptic peptides generated in Proteome Discoverer. For each identified

semi-tryptic peptide in the PP experiment a ratio of the observed reporter ion intensities in the (+) ligand samples (Cu, PT, PT + Cu, and PcephPT + Cu treated) to the (-) ligand sample (untreated) was generated for each biological replicate. The resulting ratio was divided by the normalization factor for each of the four biological replicates. Due to the nature of the experiment and the possibility of expression level changes during cell treatment, changes in the levels of semi-tryptic peptides could be falsely identified as changes due to protein stability when they are in fact due to changes in protein expression. Therefore, the semi-tryptic peptide ratios generated above were divided by the protein expression ratio generated for that protein under the corresponding conditions. These final protein expression-normalized semi-tryptic peptide stability ratios (fold change) were then log₂-base transformed, averaged, and subjected to a two-tailed Student's *t*-test comparing with a mean of zero. The log₂(fold change) values of all the semi-tryptic peptides for each comparison were used to calculate the mean log₂(fold change) and standard deviation (σ) of its distribution. Hit peptides were identified based on two criteria, (i) the peptide must have a significantly altered log₂(fold change) value ($\geq 2\sigma$ deviations from mean log₂(fold change)); and (ii) the log₂(fold change) value must be significantly different from zero, as determined by a Student's two-tailed *t*-test (p -value ≤ 0.05).

Fuzzy c-means cluster analysis. Fuzzy c-means clustering is a soft clustering method first reported by Dunn in 1974.⁷ It is commonly used in pattern recognition, in which clusters are found based on the distance or similarity of points to each other. In soft clustering methods, a data point can be a member of all the clusters or patterns identified from a data set by attributing each data point with a membership score ranging from 0 to 1. The points closer to the center of a specific cluster will have a higher membership score of belonging to that cluster. Fuzzy c-means clustering was performed in R Studio (3.6.0 (2019-04-26) – "Planting of a Tree") using the "ppclust" package. The log₂(fold change) intensities of each the 407 peptide stability hits were scaled from 0 to 1 across the four treatment conditions compared to untreated. This scaling enabled the clustering method to search for trends across treatment conditions and not group peptides based on the magnitudes of their stability changes, which could be misleading. FCM was setup using the function *fcm* with 4 initial cluster centers (centers = 4) and allowed to start and iterate to a final solution ten times (nstart = 10). The output of the most optimal solution was used to group protein hits into the four clusters. Membership scores (ranging from 0 to 1) indicating how well a peptide fits into each cluster, were exported for each peptide stability hit, and peptides with scores ≥ 0.7 were considered as being confidently classified into one of the four clusters. Using this cutoff, ~70% of protein hits were classified into the four clusters.

Enzyme activity assays. For assays evaluating enzyme activity in treated bacteria, *E. coli* MG1655 expressing CTX-M-1 was grown to an OD₆₀₀ of 0.1–0.2, treated for 15 min, pelleted, and washed twice with 5 mL of water. The resulting pellets (100 mL cell suspension per pellet) were frozen at -20 °C for later use. Each treated pellet was lysed within 30 min of starting the activity assay in order to prevent loss of activity due to exposure to air. Pellets were lysed on ice by sonication (six cycles, 10 s pulse at 30% amplitude with 50 s rest) in 200 μ L buffer (for GAPDH, 50 mM sodium phosphate buffer, pH 7.5; for IDH, 50 mM Tris buffer, pH 7.4) and centrifuged at 14,000 g for 10 min. The resulting supernatant was diluted in the appropriate buffer to make a lysate working solution (for GAPDH, 1:50 in sodium phosphate buffer; for IDH, 1:10 in Tris buffer), which was then added to a quartz cuvette containing the appropriate assay mix. The GAPDH assay mix contained 50 mM sodium phosphate buffer (pH 7.5), 5 mM EDTA, 40 mM triethanolamine, and 2 mM NAD⁺. The IDH assay mix contained 50 mM Tris buffer (pH 7.4) and 0.2 mM NADP⁺. Lysate working solution (25 μ L) was added to the cuvette, vortexed, and used to

blank the UV-Vis. Activity was assessed by monitoring the appearance of NADH or NADPH at 340 nm every 2 min for 30 min following addition of the appropriate substrate. Spectra were collected in a quartz cuvette with 1 cm pathlength using a Varian Cary 50 UV-visible spectrophotometer. The final concentration of substrate was 2 mM DL-glyceraldehyde-3-phosphate for the GAPDH assay and 10 mM isocitrate for the IDH assay. Total reaction volume in the cuvette was 250 μ L. For all enzyme activity experiments, treated data were normalized to protein concentration and the A_{340} of the untreated condition at 30 min. At least two biological replicates were performed.

For purified GAPDH, 0.254 μ M purified GAPDH was incubated for 20 min with various concentrations of Cu in 50 mM sodium phosphate buffer (pH 7.5). A 25- μ L aliquot of treated enzyme was added to a quartz cuvette containing GAPDH assay mix as described above, vortexed, and used to blank the UV-Vis. Then 2 mM DL-glyceraldehyde-3-phosphate was added (250 μ L total reaction volume) and the absorbance at 340 nm was measured every 2 min for 30 min. For purified IDH, 31.8 μ M purified IDH was incubated for 20 min with various concentrations of Cu in 50 mM Tris buffer (pH 7.4). A 25- μ L aliquot of treated enzyme was added to a quartz cuvette containing IDH assay mix as described above, vortexed, and used to blank the UV-Vis. Then 10 mM isocitrate was added (250 μ L total reaction volume) and the absorbance at 340 nm was measured every 2 min for 30 min. At least three replicates from different days were performed for purified enzyme activity assays.

Circular dichroism spectroscopy. Circular dichroism spectra were obtained on an Aviv model 435 circular dichroism spectrometer equipped with a Hamilton automated titrator. The purified GAPDH CD denaturation curves were monitored at 217 nm. The CD denaturation points were set up and recorded using the automatic titration system connected to the CD instrument. In each titration, different amounts of 0 and 8–9 M urea solutions containing purified GAPDH (~0.1 mg/mL, 2.8–3.1 μ M) with and without CuCl_2 (100 μ M) in phosphate buffer (pH 7.4) were mixed in different ratios to obtain the final desired urea concentration for each point. The mixing time was 1 min, CD signals were collected over the course of 5 s, and the signals were averaged. The averaged CD signals were plotted and normalized to pre- and post-transition baselines to obtain final normalized denaturation curves (F_{app}) of GAPDH in the presence and absence of Cu^{2+} . The normalized denaturation curves were fit to a simple four point sigmoidal to estimate midpoint values. The purified IDH CD spectra were obtained over a wavelength range of 215–240 nm. A solution of IDH (0.1 mg/mL, 2.2 μ M) was incubated with and without CuCl_2 (100 μ M) in phosphate buffer (pH 7.4). The solutions were allowed to sit overnight before taking the measurements. The CD signal was converted from ellipticity (in millidegrees) to molar ellipticity using the following equation:

$$[\theta] = \frac{m^o \times M}{10 \times C \times l}$$

Where, m^o is ellipticity in millidegrees, M is the average molecular weight of the protein (36,000 g/mol for GAPDH, 58,000 g/mol for IDH), C is the concentration of the sample in mg/mL, and l is the pathlength in cm.

Safety Statement. No unexpected or unusually high safety hazards were encountered.

References

1. Zaengle-Barone, J. M. *et al.* Copper Influences the Antibacterial Outcomes of a β -Lactamase-Activated Prochelator against Drug-Resistant Bacteria. *ACS Infect. Dis.* **4**, 1019–1029 (2018).
2. Volkmer, B. & Heinemann, M. Condition-Dependent Cell Volume and Concentration of *Escherichia coli* to Facilitate Data Conversion for Systems Biology Modeling. *PLoS ONE* **6**, (2011).
3. Ma, R., Meng, H., Wiebelhaus, N. & Fitzgerald, M. C. Chemo-Selection Strategy for Limited Proteolysis Experiments on the Proteomic Scale. *Anal. Chem.* **90**, 14039–14047 (2018).
4. Cabrera, A. *et al.* Comparative Analysis of Mass-Spectrometry-Based Proteomic Methods for Protein Target Discovery Using a One-Pot Approach. *J. Am. Soc. Mass Spectrom.* **31**, 217–226 (2020).
5. Perez-Riverol, Y. *et al.* The PRIDE database and related tools and resources in 2019: improving support for quantification data. *Nucleic Acids Res.* **47**, D442–D450 (2019).
6. Deutsch, E. W. *et al.* The ProteomeXchange consortium in 2020: enabling 'big data' approaches in proteomics. *Nucleic Acids Res.* **48**, D1145–D1152 (2020).
7. Dunn, J. C. Well-Separated Clusters and Optimal Fuzzy Partitions. *J. Cybern.* **4**, 95–104 (1974).

Supplementary Table 1 | Proteomic coverage from protein expression level and protein stability analyses. Number of proteins and peptides assayed in the expression and stability analyses, respectively, along with the number of hit proteins and peptides under each condition (i.e. those with significant changes in their expression or stability according to the hit criteria).

Treatment condition	Protein expression		Protein stability	
	Assayed proteins	Hit proteins	Assayed peptides (proteins)	Hit peptides (proteins)
Cu	898	8	4605 (584)	55 (37)
PT	898	36	4605 (584)	167 (69)
Cu + PcephPT	898	20	4605 (584)	170 (84)
Cu + PT	898	24	4605 (584)	144 (74)

Supplementary Table 2 | Complete list of protein expression level hits. Cumulative list of protein hits with significant treatment-induced expression level changes identified in this work.

Accession number	Protein name	Gene code
P25516	Aconitate hydratase A	acnA
P0A9Q9	Aspartate-semialdehyde dehydrogenase	asd
P0ABH9	ATP-dependent Clp protease ATP-binding subunit ClpA	clpA
P63284	Chaperone protein ClpB	clpB
Q59385	Copper-exporting P-type ATPase	copA
P24251	Sigma factor-binding protein Crl	crl
P36649	Blue copper oxidase CueO	cueO
P0ABJ1	Cytochrome bo(3) ubiquinol oxidase subunit 2	cyoA
P0ABK5	Cysteine synthase A	cysK
P16703	Cysteine synthase B	cysM
P0A6K3	Peptide deformylase	def
P0A6Y8	Chaperone protein DnaK	dnaK
P0ADI4	Enterobactin synthase component B	entB
P0AEJ2	Isochorismate synthase EntC	entC
P11454	Enterobactin synthase component F	entF
P75780	Catecholate siderophore receptor Fiu	fiu
P05042	Fumarate hydratase class II	fumC
P09148	Galactose-1-phosphate uridylyltransferase	galT
P33195	Glycine dehydrogenase (decarboxylating)	gcvP
P27248	Aminomethyltransferase	gcvT
P68066	Autonomous glycy radical cofactor	grcA
P0A6F9	10 kDa chaperonin	groS
P68688	Glutaredoxin 1	grxA
P04425	Glutathione synthetase	gshB
P60560	GMP reductase	guaC
P0A6Z3	Chaperone protein HtpG	htpG
P0C054	Small heat shock protein IbpA	ibpA
P0C058	Small heat shock protein IbpB	ibpB
P27294	Protein InaA	inaA
P0AAC8	Iron-binding protein IscA	iscA
P0AGK8	HTH-type transcriptional regulator IscR	iscR
P0A6B7	Cysteine desulfurase IscS	iscS
P0ACD4	Iron-sulfur cluster assembly scaffold protein IscU	iscU
P13029	Catalase-peroxidase	katG
P0A725	UDP-3-O-acyl-N-acetylglucosamine deacetylase	lpxC
P0AEY5	Modulator of drug activity B	mdaB
P0AF18	N-acetylglucosamine-6-phosphate deacetylase	nagA
P77258	N-ethylmaleimide reductase	nema
P17117	Oxygen-insensitive NADPH nitroreductase	nfsA
P38489	Oxygen-insensitive NAD(P)H nitroreductase	nfsB

P52697	6-phosphogluconolactonase	pgl
P0A9J8	Bifunctional chorismate mutase/prephenate dehydratase	pheA
P0C037	Pyrimidine/purine nucleoside phosphorylase	ppnP
P36999	23S rRNA (guanine(745)-1-methyltransferase	rlmA
P0A7P5	50S ribosomal protein L34	rpmH
P0A9T0	D-3-phosphoglycerate dehydrogenase	serA
P27306	Soluble pyridine nucleotide transhydrogenase	sthA
P0A9T4	Protein tas	tas
P0A877	Tryptophan synthase alpha chain	trpA
P33030	Zinc-binding GTPase YeiR	yeiR
P0ADV5	Luciferase-like monooxygenase	yhbW
P76116	Uncharacterized protein YncE	yncE
P37617	Zinc/cadmium/lead-transporting P-type ATPase	zntA

Supplementary Table 3 | Complete list of protein stability hits. Cumulative list of protein hits with significant treatment-induced stability changes identified in this work.

Accession number	Protein name	Gene code
P0ABD8	Biotin carboxyl carrier protein of acetyl-CoA carboxylase	accB
P08997	Malate synthase A	aceB
P0AFG8	Pyruvate dehydrogenase E1 component	aceE
P06959	Dihydrolipoyllysine-residue acetyltransferase component of pyruvate dehydrogenase complex	aceF
P0A6A3	Acetate kinase	ackA
P25516	Aconitate hydratase A	acnA
P36683	Aconitate hydratase B	acnB
P0A6A8	Acyl carrier protein	acpP
P0AE08	Alkyl hydroperoxide reductase C	ahpC
P35340	Alkyl hydroperoxide reductase subunit F	ahpF
P0A6D7	Shikimate kinase 1	aroK
P0A9Q9	Aspartate-semialdehyde dehydrogenase	asd
P0A8M0	Asparagine--tRNA ligase	asnS
P0ABB4	ATP synthase subunit beta	atpD
P17445	NAD/NADP-dependent betaine aldehyde dehydrogenase	betB
P63284	Chaperone protein ClpB	clpB
Q59385	Copper-exporting P-type ATPase	copA
P0A9X9	Cold shock protein CspA	cspA
P0A972	Cold shock-like protein CspE	cspE
P36649	Blue copper oxidase CueO	cueO
P0ABK5	Cysteine synthase A	cysK
P0AEB2	D-alanyl-D-alanine carboxypeptidase DacA	dacA
P0A6K3	Peptide deformylase	def
P0A6Y8	Chaperone protein DnaK	dnaK
P0A953	3-oxoacyl-[acyl-carrier-protein] synthase 1	fabB
P0AEK4	Enoyl-[acyl-carrier-protein] reductase [NADH] FabI	fabI
P0A805	Ribosome-recycling factor	frf
P0AAB6	UTP--glucose-1-phosphate uridylyltransferase	galF
P0A9B2	Glyceraldehyde-3-phosphate dehydrogenase A	gapA
P00960	Glycine--tRNA ligase alpha subunit	glyQ
P62707	2,3-bisphosphoglycerate-dependent phosphoglycerate mutase	gpmA
P37689	2,3-bisphosphoglycerate-independent phosphoglycerate mutase	gpmI
P68066	Autonomous glycyl radical cofactor	grcA
P0A6F5	60 kDa chaperonin	groL
P0A6F9	10 kDa chaperonin	groS
P09372	Protein GrpE	grpE
P68688	Glutaredoxin 1	grxA
P0AC62	Glutaredoxin 3	grxC
P0AC69	Glutaredoxin 4	grxD
P04425	Glutathione synthetase	gshB

P60560	GMP reductase	guaC
P0ACB2	Delta-aminolevulinic acid dehydratase	hemB
P67910	ADP-L-glycero-D-manno-heptose-6-epimerase	hldD
P0ACF8	DNA-binding protein H-NS	hns
P0A9M2	Hypoxanthine phosphoribosyltransferase	hpt
P0A6Z1	Chaperone protein HscA	hscA
P0A6H5	ATP-dependent protease ATPase subunit HslU	hslU
P0A7B8	ATP-dependent protease subunit HslV	hslV
P0A6Z3	Chaperone protein HtpG	htpG
P0ACF0	DNA-binding protein HU-alpha	hupA
P0C054	Small heat shock protein IbpA	ibpA
P0C058	Small heat shock protein IbpB	ibpB
P08200	Isocitrate dehydrogenase [NADP]	icd
P27294	Protein InaA	inaA
P0A705	Translation initiation factor IF-2	infB
P0AGK8	HTH-type transcriptional regulator IscR	iscR
P0A6B7	Cysteine desulfurase IscS	iscS
P60716	Lipoyl synthase	lipA
P0A9M0	Lon protease	lon
P0A8N3	Lysine--tRNA ligase	lysS
P26616	NAD-dependent malic enzyme	maeA
P0AE18	Methionine aminopeptidase	map
P61889	Malate dehydrogenase	mdh
P0A817	S-adenosylmethionine synthase	metK
P09424	Mannitol-1-phosphate 5-dehydrogenase	mtlD
P0AFF6	Transcription termination/antitermination protein NusA	nusA
P31663	Pantothenate synthetase	panC
P22259	Phosphoenolpyruvate carboxykinase (ATP)	pckA
P37095	Peptidase B	pepB
P15288	Cytosol non-specific dipeptidase	pepD
P04825	Aminopeptidase N	pepN
P09373	Formate acetyltransferase 1	pflB
P05055	Polyribonucleotide nucleotidyltransferase	pnp
P00864	Phosphoenolpyruvate carboxylase	ppc
P0A7I4	Peptide chain release factor RF3	prfC
P45577	RNA chaperone ProQ	proQ
P0AFM2	Glycine betaine/proline betaine-binding periplasmic protein	proX
P0A9M8	Phosphate acetyltransferase	pta
P08839	Phosphoenolpyruvate-protein phosphotransferase	ptsl
P0A7D4	Adenylosuccinate synthetase	purA
P0AD61	Pyruvate kinase I	pykF
P0AG30	Transcription termination factor Rho	rho
P0A7J0	3,4-dihydroxy-2-butanone 4-phosphate synthase	ribB
P0AFU8	Riboflavin synthase	ribC
P61714	6,7-dimethyl-8-ribityllumazine synthase	ribE

P0AEI4	Ribosomal protein S12 methylthiotransferase RimO	rimO
P0C0R7	Ribosomal RNA large subunit methyltransferase E	rlmE
P0A7L0	50S ribosomal protein L1	rplA
P60422	50S ribosomal protein L2	rplB
P60438	50S ribosomal protein L3	rplC
P60723	50S ribosomal protein L4	rplD
P62399	50S ribosomal protein L5	rplE
P0AG55	50S ribosomal protein L6	rplF
P0A7R1	50S ribosomal protein L9	rplI
P0A7J3	50S ribosomal protein L10	rplJ
P0A7J7	50S ribosomal protein L11	rplK
P0ADY3	50S ribosomal protein L14	rplN
P02413	50S ribosomal protein L15	rplO
P0AG44	50S ribosomal protein L17	rplQ
P0C018	50S ribosomal protein L18	rplR
P0A7K6	50S ribosomal protein L19	rplS
P0A7L3	50S ribosomal protein L20	rplT
P61175	50S ribosomal protein L22	rplV
P0ADZ0	50S ribosomal protein L23	rplW
P60624	50S ribosomal protein L24	rplX
P68919	50S ribosomal protein L25	rplY
P0A7L8	50S ribosomal protein L27	rpmA
P0A7M2	50S ribosomal protein L28	rpmB
P0AG51	50S ribosomal protein L30	rpmD
P0A7M9	50S ribosomal protein L31	rpmE
P0A7N9	50S ribosomal protein L33	rpmG
P0A7P5	50S ribosomal protein L34	rpmH
P0A7Z4	DNA-directed RNA polymerase subunit alpha	rpoA
P0A8V2	DNA-directed RNA polymerase subunit beta	rpoB
P0A8T7	DNA-directed RNA polymerase subunit beta'	rpoC
P0AG67	30S ribosomal protein S1	rpsA
P0A7V0	30S ribosomal protein S2	rpsB
P0A7V3	30S ribosomal protein S3	rpsC
P0A7V8	30S ribosomal protein S4	rpsD
P0A7W1	30S ribosomal protein S5	rpsE
P02358	30S ribosomal protein S6	rpsF
P02359	30S ribosomal protein S7	rpsG
P0A7W7	30S ribosomal protein S8	rpsH
P0A7X3	30S ribosomal protein S9	rpsI
P0A7R5	30S ribosomal protein S10	rpsJ
P0A7R9	30S ribosomal protein S11	rpsK
P0A7S3	30S ribosomal protein S12	rpsL
P0A7S9	30S ribosomal protein S13	rpsM
P0AG59	30S ribosomal protein S14	rpsN
P0ADZ4	30S ribosomal protein S15	rpsO

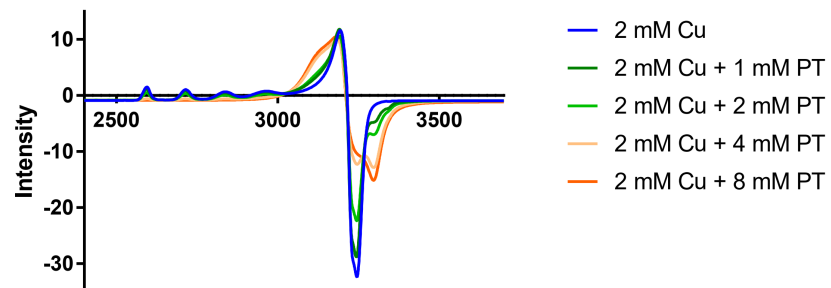
P0AG63	30S ribosomal protein S17	rpsQ
P0A7U7	30S ribosomal protein S20	rpsT
P68679	30S ribosomal protein S21	rpsU
P0AC41	Succinate dehydrogenase flavoprotein subunit	sdhA
P0AG86	Protein-export protein SecB	secB
P16456	Selenide, water dikinase	selD
P0A8L1	Serine--tRNA ligase	serS
P0A9K9	FKBP-type peptidyl-prolyl cis-trans isomerase SlyD	slyD
P0ACG1	DNA-binding protein StpA	stpA
P0AFG3	2-oxoglutarate dehydrogenase E1 component	sucA
P0AFG6	Dihydrolipoyllysine-residue succinyltransferase component of 2-oxoglutarate dehydrogenase complex	sucB
P69428	Sec-independent protein translocase protein Tata	tatA
P0A8M3	Threonine--tRNA ligase	thrS
P0A850	Trigger factor	tig
P0A853	Tryptophanase	tnaA
P0A862	Thiol peroxidase	tpx
P0A6P1	Elongation factor Ts	tsf
P0A890	Sulfur carrier protein TusA	tusA
P07118	Valine--tRNA ligase	valS
P0A8J4	UPF0250 protein YbeD	ybeD
P0A9U3	Uncharacterized ABC transporter ATP-binding protein YbiT	ybiT
P29217	UPF0502 protein YceH	yceH
P0ABU2	Ribosome-binding ATPase YchF	ychF
P0A8M6	UPF0265 protein YeeX	yeeX
P0A6N8	Elongation factor P-like protein	yeiP
P0ADV5	Luciferase-like monooxygenase	yhbW
P76116	Uncharacterized protein YncE	yncE
Q46856	Alcohol dehydrogenase YqhD	yqhD
P37617	Zinc/cadmium/lead-transporting P-type ATPase	zntA

Supplementary Table 4 | Biological process classification of protein stability hits. Stability hit peptides in each condition were sorted into categories based on their GO biological process terms extracted using DAVID functional analysis and more generally classified into GO Term categories.

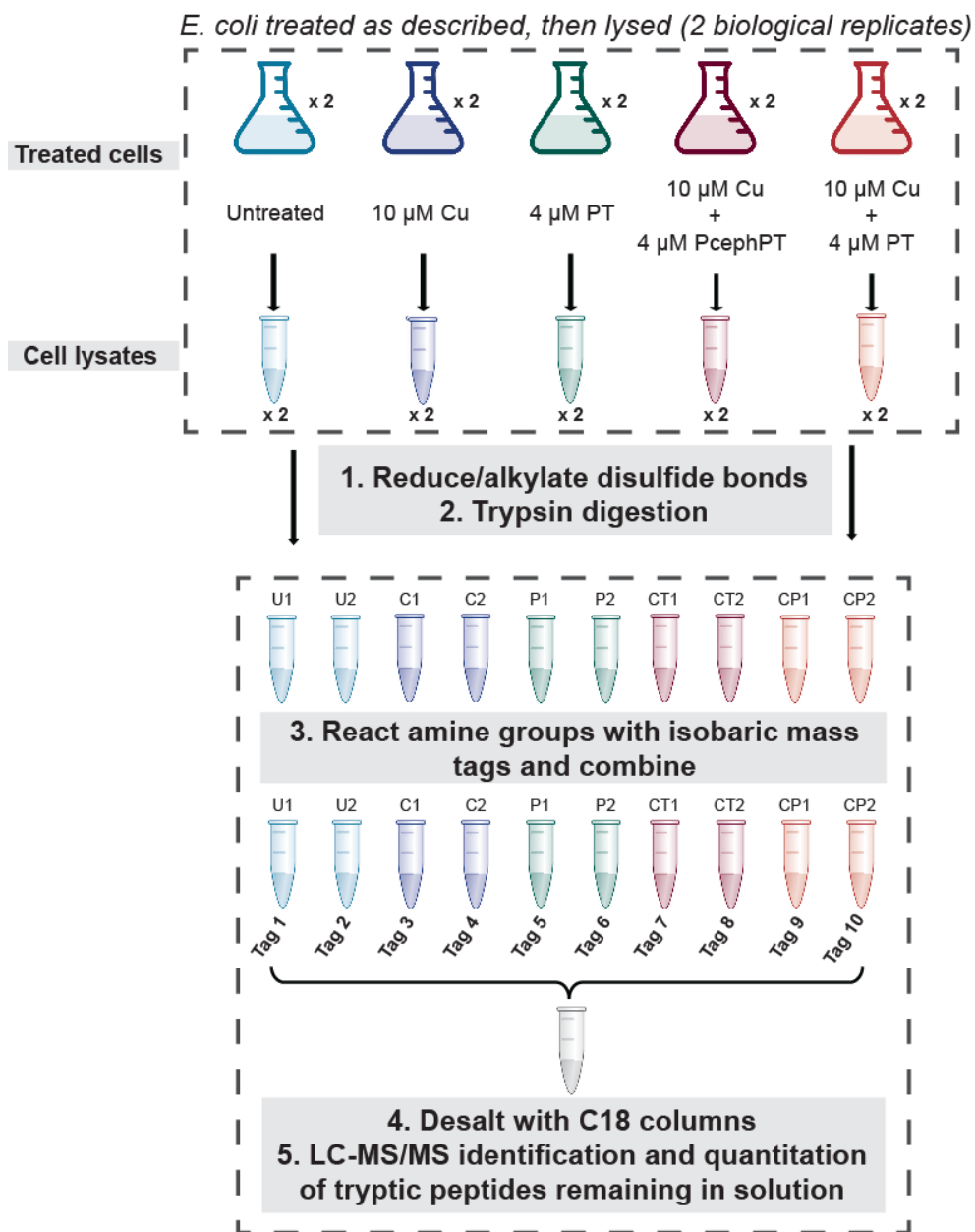
Category	# of hit peptides (proteins)				
	Cu	PT	Cu + PcephPT	Cu + PT	Total
Metal detoxification	5 (2)	5 (3)	4 (2)	7 (3)	8 (3)
Fe-S cluster synthesis	1 (1)	3 (1)	3 (1)	2 (1)	5 (2)
Glycolysis and TCA cycle	4 (4)	10 (7)	8 (7)	15 (8)	28 (15)
Biosynthetic processes	3 (3)	15 (9)	6 (5)	12 (11)	31 (23)
Metabolic processes (other)	3 (3)	4 (3)	4 (4)	7 (5)	14 (12)
Transcription	14 (6)	18 (5)	15 (7)	14 (6)	36 (11)
Translation (ribosome)	18 (11)	49 (21)	114 (36)	58 (21)	170 (44)
Translation (other)	2 (2)	1 (1)	11 (9)	5 (4)	16 (13)
Unfolded protein response	1 (1)	55 (6)	3 (3)	10 (5)	60 (10)
Peptide degradation	0 (0)	8 (4)	3 (2)	7 (3)	9 (4)
Cell redox homeostasis	1 (1)	4 (3)	3 (2)	8 (5)	13 (8)
Stress response	2 (2)	5 (3)	1 (1)	1 (1)	8 (5)
Other/unknown classification	1 (1)	3 (3)	5 (5)	1 (1)	9 (9)
Total hits	55 (37)	180 (69)	180 (84)	147 (74)	407 (159)

Supplementary Table 5 | Biological process classification of protein stability hits within each cluster. Stability hit peptides within each cluster were sorted into categories based on their GO biological process terms extracted using DAVID functional analysis and more generally classified into GO Trim term categories.

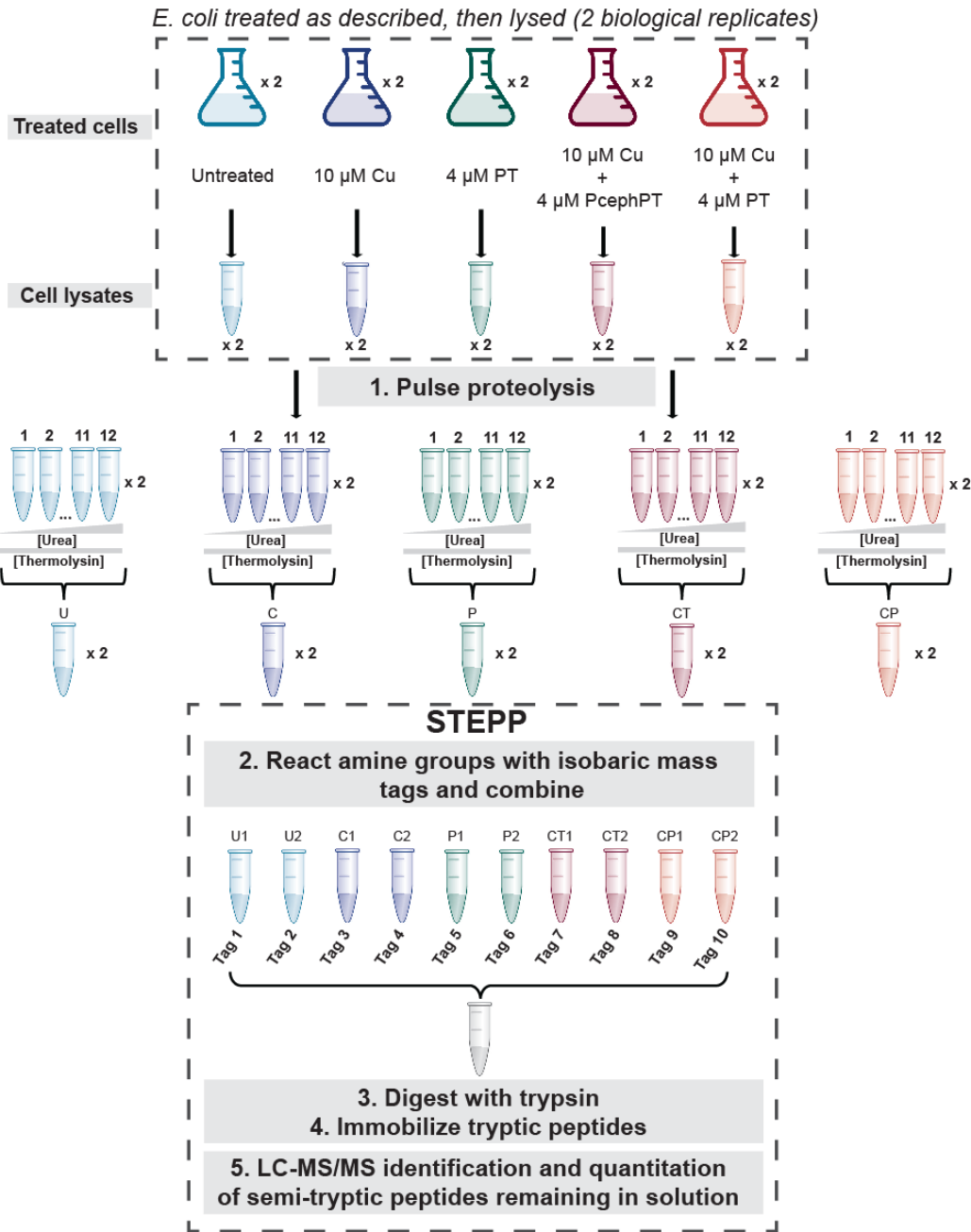
Cluster	# of hit peptides (proteins)				Total classified
	Cluster 1 (Cu-Driven, Stab.)	Cluster 2 (PcephPT-Driven, Destab.)	Cluster 3 (PT-Driven, Stab.)	Cluster 4 (PT-Driven, Destab.)	
Metal detoxification	2 (1)	0 (0)	1 (1)	0 (0)	3 (2)
Fe-S cluster synthesis	0 (0)	0 (0)	0 (0)	1 (1)	1 (1)
Glycolysis and TCA cycle	10 (6)	3 (3)	1 (1)	2 (2)	16 (11)
Biosynthetic processes	2 (2)	3 (3)	4 (3)	6 (5)	15 (13)
Metabolic processes (other)	0 (0)	2 (2)	0 (0)	2 (2)	4 (4)
Transcription	2 (2)	7 (6)	7 (1)	2 (2)	18 (9)
Unfolded protein response	2 (2)	2 (2)	36 (3)	1 (1)	41 (7)
Peptide degradation	1 (1)	0 (0)	4 (3)	0 (0)	5 (3)
Translation (ribosome)	28 (10)	61 (18)	2 (2)	23 (13)	114 (34)
Translation (other)	4 (3)	8 (6)	0 (0)	1 (1)	13 (10)
Cell redox homeostasis	5 (4)	1 (1)	3 (2)	0 (0)	9 (7)
Stress response	0 (0)	1 (1)	2 (1)	2 (2)	5 (3)
Other/unknown classification	0 (0)	3 (3)	1 (1)	1 (1)	5 (5)
Total hits	56 (31)	91 (46)	61 (18)	41 (30)	249 (109)



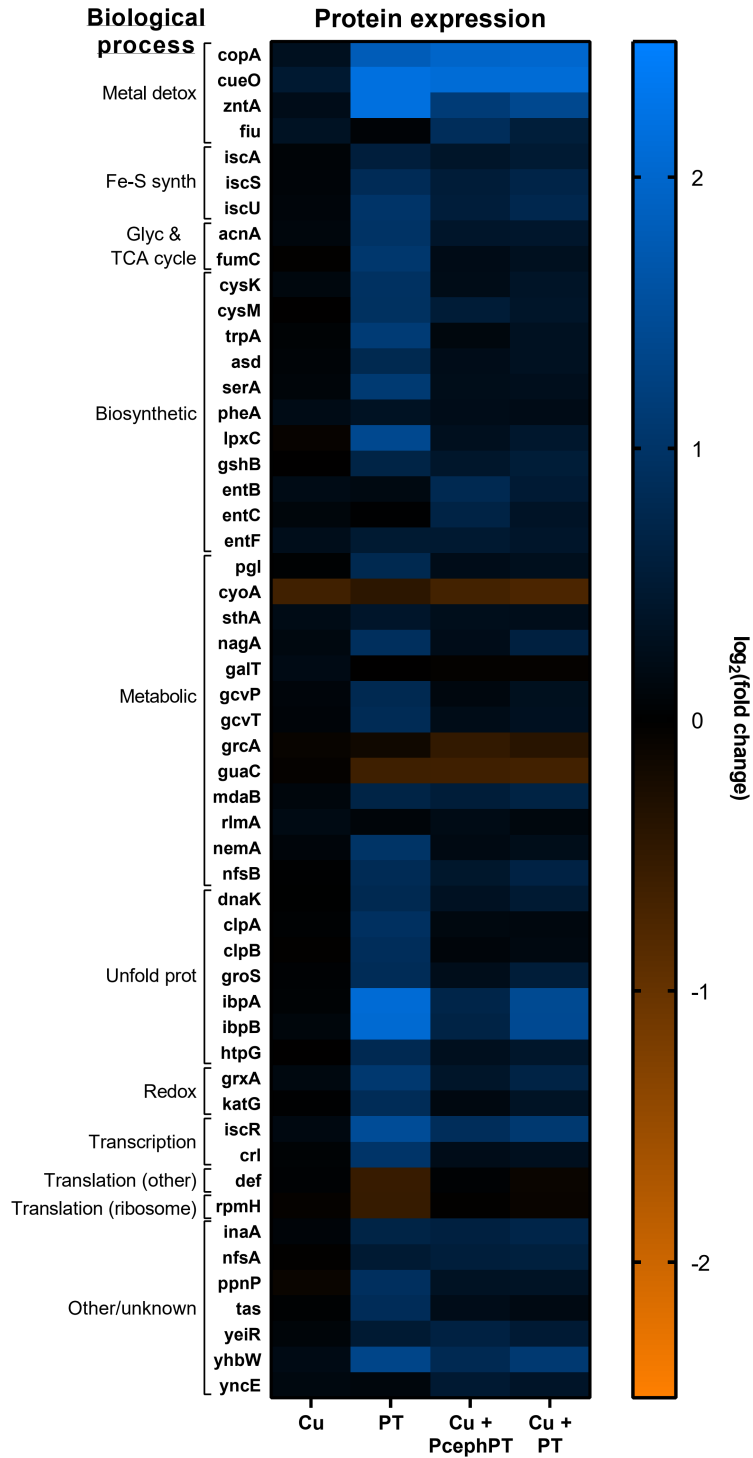
Supplementary Figure 1 | Electron paramagnetic resonance spectroscopy of Cu titrated with PT in 10% glycerol.



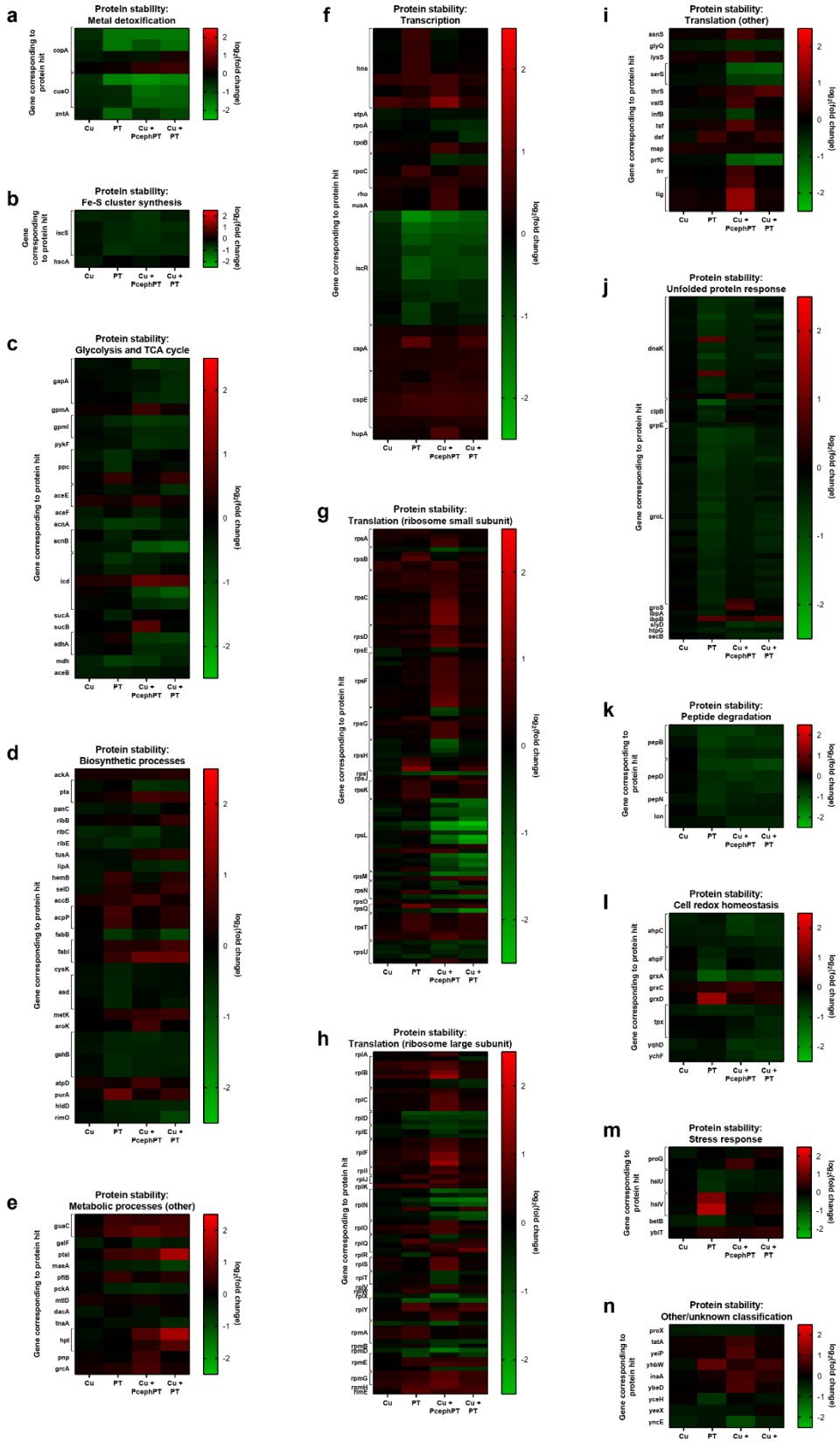
Supplementary Figure 2 | Experimental workflow and isobaric mass tagging scheme for protein expression analysis. The above workflow was performed twice to generate a total of four biological replicates.



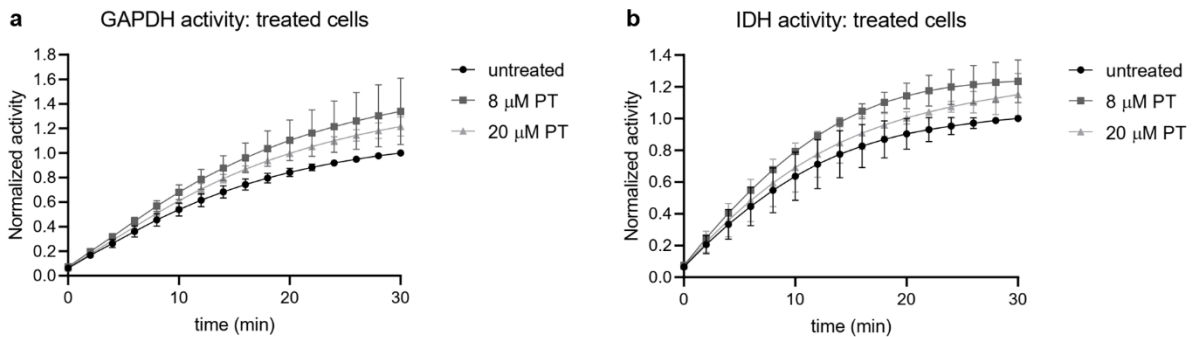
Supplementary Figure 3 | Experimental workflow and isobaric mass tagging scheme for protein stability analysis. The above workflow was performed twice to generate a total of four biological replicates.



Supplementary Figure 4 | Heat map visualizing magnitude of expression changes for hit proteins grouped by biological process. Heat map displaying the log₂(fold change) in expression level of proteins that were hits in at least one treatment condition. The same data are shown in the volcano plot (**Figure 3**). Positive values (blue) indicate increased expression, while negative values (orange) indicate decreased expression compared to the untreated condition. Proteins are identified by their corresponding gene codes.



Supplementary Figure 5 | Heat maps visualizing magnitude of stability changes for hit peptides grouped by biological process. Heat maps displaying the $\log_2(\text{fold change})$ in stability of peptides that were hits in at least one treatment condition. Negative values (green) indicate increased stability, while positive values (red) indicate decreased stability compared to the untreated condition. Proteins are identified by their corresponding gene codes.



Supplementary Figure 6 | GAPDH and IDH activity in cells treated with PT. **a**, Activity of GAPDH measured in cell lysates of *E. coli* treated for 15 min as indicated; **b**, activity of IDH measured in cell lysates of *E. coli* treated for 15 min as indicated.